Remote Sensing of Environment 136 (2013) 330–341

Contents lists available at SciVerse ScienceDirect

Remote Sensing of Environment

journal homepage: www.elsevier.com/locate/rse

A comparison of foliage profiles in the Sierra National Forest obtained with a full-waveform under-canopy EVI lidar system with the foliage profiles obtained with an airborne full-waveform LVIS lidar system

Feng Zhao [a,b,*], Xiaoyuan Yang [c,a], Alan H. Strahler [a], Crystal L. Schaaf [c,a], Tian Yao [a], Zhuosen Wang [c,a], Miguel O. Román [d], Curtis E. Woodcock [a], Wenge Ni-Meister [e], David L.B. Jupp [f], Jenny L. Lovell [g], Darius S. Culvenor [h], Glenn J. Newnham [i], Hao Tang [b], Ralph O. Dubayah [b]

[a] Department of Earth and Environment, Boston University, Boston, MA 02215, USA
[b] Department of Geographical Sciences, University of Maryland, College Park, MD 20742, USA
[c] Environmental Earth and Ocean Sciences, University of Massachusetts, Boston, MA 02125, USA
[d] Terrestrial Information Systems Laboratory (Code 619), NASA Goddard Space Flight Center, Greenbelt, MD 20705, USA
[e] Department of Geography, Hunter College of CUNY, New York, NY 10065, USA
[f] CSIRO Marine and Atmospheric Research, Canberra, ACT 2601, Australia
[g] CSIRO Marine and Atmospheric Research, Hobart, TAS 7000, Australia
[h] Environmental Sensing Systems, Melbourne, Australia
[i] CSIRO Land and Water, Clayton, Victoria 3169, Australia

ARTICLE INFO

Article history:
Received 26 November 2012
Received in revised form 8 May 2013
Accepted 11 May 2013
Available online xxxx

Keywords:
Foliage profile
Ground-based full-waveform lidar
Airborne full-waveform lidar system
EVI
LVIS

ABSTRACT

Foliage profiles retrieved from a scanning, terrestrial, near-infrared (1064 nm), full-waveform lidar, the Echidna Validation Instrument (EVI), agree well with those obtained from an airborne, near-infrared, full-waveform, large footprint lidar, the Lidar Vegetation Imaging Sensor (LVIS). We conducted trials at 5 plots within a conifer stand at Sierra National Forest in August, 2008. Foliage profiles retrieved from these two lidar systems are closely correlated (e.g., $r = 0.987$ at 100 m horizontal distances) at large spatial coverage while they differ significantly at small spatial coverage, indicating the apparent scanning perspective effect on foliage profile retrievals. Also we noted the obvious effects of local topography on foliage profile retrievals, particularly on the topmost height retrievals. With a fine spatial resolution and a small beam size, terrestrial lidar systems complement the strengths of the airborne lidars by making a detailed characterization of the crowns from a small field site, and thereby serving as a validation tool and providing localized tuning information for future airborne and spaceborne lidar missions.

Published by Elsevier Inc.

1. Introduction

The vertical distribution of foliage area per unit volume above the ground, referred to as the foliage profile, shows great promise and capacity for the estimation of aboveground biomass (Drake et al., 2002; Lefsky et al., 1999; Stark et al., 2012), for the distribution of transmitted directed light inside the canopy (Parker et al., 2001), and for the estimation of gross primary productivity (GPP) and net primary productivity (NPP) (Kotchenova et al., 2004; Toda et al., 2009). However, direct ground measurements of the vertical foliage distribution, such as with stratified clipping of biomass samples, are generally destructive, time consuming and labor intensive. Similarly, indirect techniques such as the point-quadrat method (Wilson, 1960, 1963, 1965) are also laborious and time consuming, especially at the forest stand scale. As a result, considerable research has been devoted to measuring foliage profiles with remote sensing approaches that are particularly suited for large-area sampling and mapping of spatially explicit estimates of foliage profiles (Harding et al., 2001; Jupp et al., 2009; Lefsky et al., 1999; Strahler et al., 2008; Tang et al., 2012; Zhao et al., 2011).

Most airborne and spaceborne optical remote sensing systems provide estimates of the horizontal distribution of canopies (e.g., Landsat, MODIS), but have difficulty in characterizing the vertical distribution of canopy elements (Harding et al., 2001; Sun et al., 2008). Only light detection and ranging (lidar) systems record the distance between the sensor and a target, and the resulting distribution of backscattered energy over height directly reflects the three dimensional vertical structure of vegetation elements. Therefore, lidar scanning systems are being widely used for foliage profile retrievals in recent studies (Harding et al., 2001; Hilker et al., 2010; Jupp et al., 2009; Lefsky et al., 1999; Strahler et al., 2008; Zhao et al., 2011). Foliage profile mapping over a large area generally requires the deployment of a discrete-return lidar scanning system or a full-waveform lidar scanning system on an airborne or

* Corresponding author at: Department of Geographical Sciences, University of Maryland, College Park, MD 20742, USA. Tel.: +1 781 475 3538.
E-mail address: fengbjfu@gmail.com (F. Zhao).

0034-4257/$ – see front matter. Published by Elsevier Inc.
http://dx.doi.org/10.1016/j.rse.2013.05.020

spaceborne platform (e.g., the airborne full-waveform lidar, Laser Vegetation Imaging Sensor (LVIS), airborne discrete-return lidar, TopEye and the spaceborne full-waveform GLAS system aboard on the Ice, Cloud, and Elevation Satellite (ICESat)). Compared with a discrete-return lidar system, a full-waveform lidar scanning system shows much greater potential for deriving information on the details of the foliage elements over height. First of all, full-waveform lidar scanning systems typically have much larger footprints (e.g. 10–60 m) that are commensurate with the scale of structure variation in the canopy (Harding et al., 2001). Second, the footprints of discrete-return lidar scanning systems are generally kept small (e.g., 10–30 cm) to focus lidar energy for higher signal-to-noise ratios in backscattered energy. As a result, depending on the sampling density of the lidar pulses, discrete-return systems may fail to characterize the lower canopy in a relative dense forest stand, or miss some tree tops.

It must be noted, however, that the ability of large-footprint, full-waveform lidar to retrieve foliage profile over sloped regions is limited, due to the complex interactions of lidar signals from vegetation and ground surface (Yang et al., 2011). Local topography affects the foliage profile retrieval directly by stretching waveforms, and the stretching effect magnifies with footprint size, slope, and off-nadir pointing angle (Lee et al., 2011). For example, within 20° of slope, given a height of roughly 25 m and a footprint size of 25 m, the errors for vegetation height range from −2 m to greater than 20 m using an extended geometric optical and radiative transfer model (Lee et al., 2011), implying that the effect of slope on foliage profiles needs to be carefully evaluated when comparing different lidar systems. Meanwhile, Ni-Meister et al. (2001) and Kotchenova et al. (2004) reported that the retrieved foliage profiles from airborne lidar scanning systems differ from the actual foliage profiles by the mean projection of normals on the direction of laser beam because the airborne system can only provide near nadir-view sampling. Therefore, foliage profiles retrieved from airborne or spaceborne platforms are generally termed as “apparent foliage profile” or “canopy height profile” while “actual foliage profile” or “foliage profile” is used for foliage profiles derived from lidar system sampling over the entire zenith region ranging from 0 to 90°.

Ground-based, full-waveform lidar scanning systems (e.g., the full-waveform lidar scanning instrument Echidna Validation Instrument (EVI)) capture both the upper hemispherical view of the canopy and the detailed description of local topography, and these systems have been used successfully to retrieve actual foliage profile retrievals (Hosoi and Omasa, 2007; Jupp et al., 2009; Strahler et al., 2008; Yao et al., 2011; Zhao et al., 2011). Such detailed characterization of forest structure from terrestrial lidar systems should provide more accurate ground-truth foliage vertical structure at the plot scale, and comparing foliage profiles retrieved from a terrestrial full-waveform lidar system with those of an airborne full-waveform lidar system would help understand the mechanism leading to the difference between apparent foliage profile and actual foliage profile, and also the effect of local topography on foliage profile retrievals. In addition, in light of the wide use of downward-scanning, full-waveform lidar systems for foliage profile retrievals, for example the airborne full-waveform Laser Vegetation Imaging Sensor (LVIS) and the spaceborne full-waveform GLAS system aboard the Ice, Cloud, and Elevation Satellite (ICESat), such a comparison of foliage profile retrievals is of particular interest.

The scanning perspective is a crucial issue in comparison between terrestrial lidar foliage profiles and airborne lidar foliage profiles primarily because terrestrial lidar systems feature a radial perspective of observations within a limited range, and thus their capability to characterize the forest is heavily influenced by the forest density as well as the sampling design used. Fig. 1a, b shows a top-down view of a point cloud for the center scan and for five merged scans for a red fir stand sampled in the Sierra National Forest. These two figures demonstrate a pattern where points are densely distributed around the center, and this density decreases gradually away from the center. Fig. 1c and d shows the point density distribution histograms corresponding to the center scan and to the five merged scans, corroborating the pattern shown in Fig. 1a, b. In contrast, the airborne lidar scanning systems are generally nadir-looking, and sample the forests in an equally spaced periodic manner. Therefore, the impact of the varying scanning perspectives on the retrieved foliage profiles must be considered when comparing results from upward- and downward-looking lidar systems.

In this study, we compare foliage profiles from a downward-looking, airborne, full-waveform lidar scanning system (i.e., LVIS) with those from an upward-looking, terrestrial, full-waveform lidar scanning system (EVI) for the foliage profiles. Specifically, we focus on 1) assessing how the foliage profile retrievals are impacted by the varying scanning perspectives of EVI and LVIS systems; 2) evaluating the effect of surface topography on the foliage profile retrievals from EVI lidar system; and 3) finally comparing the foliage profiles retrieved from the EVI and LVIS systems.

2. Methodology

2.1. Study area

Data from the EVI and from ground measurements were acquired from a high-elevation red fir stand in the Sierra National Forest, CA, in July, 2008. The sample area covers 1 ha in a square of 100 by 100 m and is subdivided into nine plots of 33×33 m^2. The sample layout was oriented in azimuth so that plot sides followed the primary directions downslope and across slope. We measured tree characteristics and leaf area index (LAI) with both the LAI-2000 and with hemispherical photos (13 observations per plot). Five EVI scans were acquired—one in the center of the center plot and four at the center of the surrounding corners of that plot (Fig. 2a). The black cross signs represent the scan positions of EVI instrument.

LVIS data were collected during September, 2008, within a few weeks of the EVI scans. LVIS Ground Elevation (LGE), LVIS Canopy Top Elevation (LCE), and LVIS Geolocated Waveform (LGW) data were downloaded from the Goddard Space Flight Center's LVIS website (lvis.gsfc.nasa.gov) (Blair et al., 2006). The “zg” (i.e., the mean elevation of the lowest mode within the waveform) field in the LGE file was used as the ground elevation for each waveform. Note that both horizontal accuracy and vertical accuracy for the sub-canopy topography were found to be approximately 2 m (1σ) for a dense, 98 to 99% closed tropical forest in Costa Rica (Blair et al., 1999).

To match the center of EVI footprints with those of LVIS over-flights in August 2008, the geographic coordinates of each EVI scanning point were recorded using a hand-hold Garmin GPSMap60 CSx with accuracy of ±10 m and then used to identify LVIS waveforms falling into the EVI ground footprints. In each ground plot, all live trees and snags 10 cm or greater in diameter at breast height (DBH) were targeted for structural measurements, including species, DBH, crown diameter, tree height, and height to the bottom of the partial crown. Fig. 2b shows a sample layout of the LVIS shots with the EVI ground point cloud as the background. The color gradient reflects the vertical height gradient of these forest plots. Note in Fig. 2b that the EVI scan center may not precisely match a single waveform, due to the inherent systematic errors of both the GPS device mounted on the LVIS system and the GPS device used to collect geographic coordinates of each EVI scanning point. (Fig. 3) provides a side view of a point cloud before slope correction and its corresponding view after slope correction.

2.2. LVIS data processing

LVIS is a full-waveform-digitizing system and records the vertical distribution of nadir-intercepted surfaces at a 30 cm vertical resolution. The LVIS instrument flew aboard the aircraft at 7 km above ground level, and recorded footprints illuminated within a ±7° field of view. For the 2008 flights, these footprints had a nominal diameter

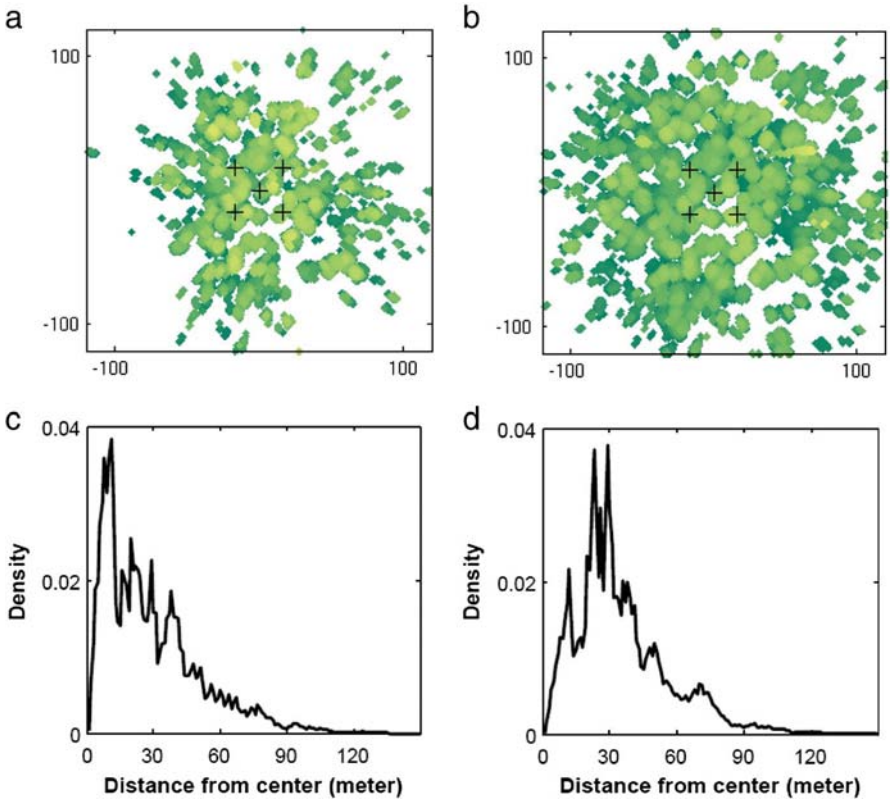

Fig. 1. Scanning perspectives of EVI data. a) A top-down view of a red fir site in the Sierra National Forest center scan; green tones from dark to light indicate heights from low to high. b) A top-down view of five merged scans. c) A histogram of point density over range for the site 305 center scan. d) A histogram of point density for the five merged scans of site 305. (For interpretation of the references to color in this figure legend, the reader is referred to the web version of this article.)

of 20 m, and therefore the canopy vertical structures should be well characterized with sufficient LVIS shots (Sun et al., 2008). The actual footprint size varies with the altitude of the aircraft, the incidence angle of the pulse, and the elevation of the target.

The methodologies for obtaining canopy height profile using airborne waveform-recording laser altimeters require a series of assumptions (Harding et al., 2001; Lefsky, 1997). First, the horizontal distribution of the canopy elements is assumed to be random with a constant leaf inclination distribution. Second, the ratio of woody to leaf surface area and the woody and leaf reflectance is constant as a function of height. Finally, multiple scattering contributes only slightly to the backscattered waveform signals. The basic steps for estimating canopy height foliage profile originated with MacArthur and Horn's (1969) method for a reflex camera with the following expression:

$$LAI_{h_2-h_1} = \frac{\ln\left(N_{h_1}/N_{h_2}\right)}{h_2-h_1} \tag{1}$$

where N_{h_1} and N_{h_2} are the number of points on which the lowest leaves are higher than h_1 and h_2, respectively, and $LAI_{h_2-h_1}$ is the leaf area density between h_1 and h_2. Given the number of points from

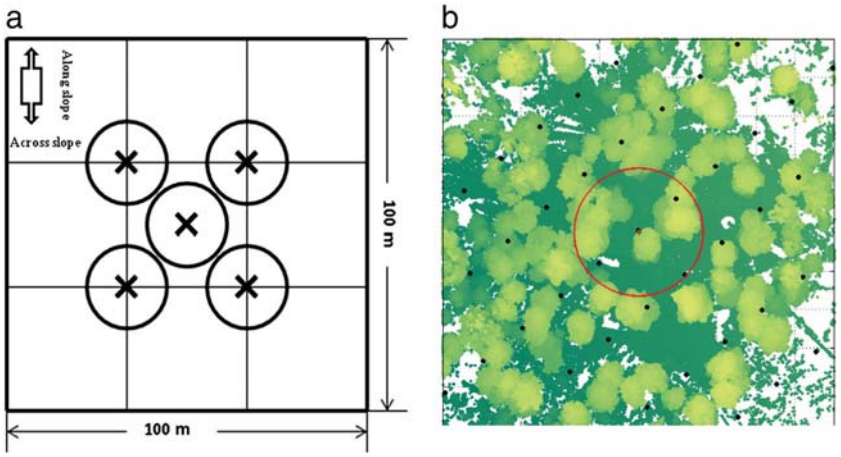

Fig. 2. a) Layout for EVI scans at Sierra National Forest; b) layout of LVIS shot center (black dots) laid upon virtual EVI center scan region of 20 m radius (red circle) with the downward view of EVI ground point cloud (dark green) at site 305 in the background. (For interpretation of the references to color in this figure legend, the reader is referred to the web version of this article.)

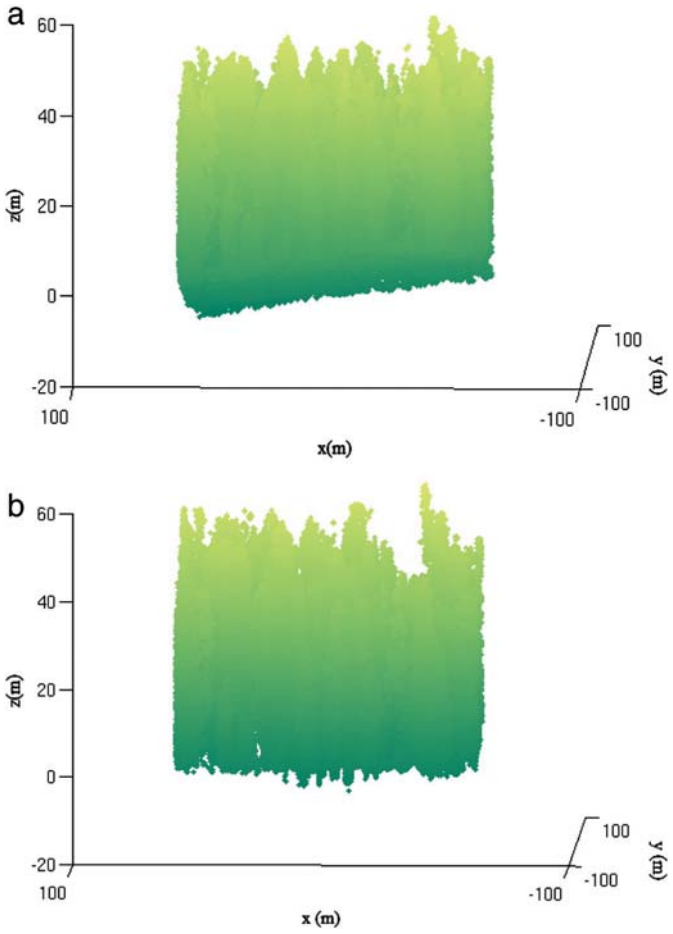

Fig. 3. EVI lidar point cloud for site 305. a) Before topographic correction; b) after topographic correction.

the ground to the top of the canopy, the foliage area volume density can be obtained by dividing the total LAI by proportion of each layer to the total. The waveform-recording laser instrument, however, measures the backscattered energy distributed over height, rather than providing the number of intercepted points, and therefore the lidar method needs adjustments for foliage area retrievals. The adjustments include smoothing the signal, identifying the background noise level, differentiating the ground and canopy returns, adjusting the return amplitude to account for difference in reflectance, computing a height distribution of canopy closure and transforming the measure to a cumulative distribution of plant material (Harding et al., 2001).

However, as mentioned, the resulting foliage profile is not exactly the actual foliage profile because it represents solely the nadir-intercepted surfaces. Ni-Meister et al. (2001) reported that the retrieved canopy height profile deviates from the actual foliage profile by the mean projection factor expressed in the following expression.

$$FHP_{retr}(z) = FHP_{act}(z)G(z,\theta_L) \tag{2}$$

where $G(z, \theta_L)$, hereafter referred to as the G function, is the mean projection of leaf normals on the direction of laser beam θ_L at height z, and $FHP_{retr}(z)$ and $FHP_{act}(z)$ are the retrieved and actual foliage area volume densities respectively. The G function varies with zenith angle, and its variation depends on the angle distribution of the facets among the scattering elements (Jupp et al., 2009). The G function is only needed for leaf area index and foliage profile retrievals when limited zeniths are sampled. When all zeniths are sampled, LAI and foliage profiles can be retrieved without specific knowledge of the G function (Jupp et al., 2009). Kotchenova et al. (2004) chose to use a field-measured canopy area index (CAI) to normalize the retrieved foliage area profile.

$$FHP(z) = (CHP_{retr}(z)/CAI_{retr})LAI \tag{3}$$

where CHP_{retr} is the retrieved canopy height profile, CAI_{retr} is the retrieved canopy height index and LAI is the field measured LAI.

In this study, raw LVIS waveforms were processed following the procedure described in Harding et al. (2001), and then the retrieved CHPs were averaged at varying spatial coverages, followed by normalization using Kotchenova's approach. All LVIS waveforms within a specified range from the EVI scanning center were extracted and added together by aligning them with waveform ground peaks, resulting in mean foliage profiles.

For the LVIS system, the height of the canopy height profile (CHP) derived from a single waveform is referenced to the start of the ground peak, and as a result, the between-footprint topography effect is minimized when several foliage profiles are averaged over an area for a mean foliage profile. However, the within-footprint topography effect remains inherent in each waveform, and cannot be removed directly. As a result, in this study, the foliage profiles retrieved from LVIS waveforms are corrected for the between-footprint effect, but still retain the within-footprint topography effect. Fig. 4 shows a DEM for site 305 interpolated from the mean elevation of the lowest mode within the waveforms recorded in the LGE file.

Locational errors associated with both the recorded geographic coordinates of the EVI scanning centers and those of LVIS waveforms using GPS devices contribute to a slight mismatch between single LVIS waveforms and EVI scanning centers. Therefore, the production of a mean foliage profile over a larger region reduces the impact of the mismatch of foliage profiles derived from upward-looking EVI and downward-looking LVIS.

To match the foliage profile from the upward-looking EVI with LVIS, we produced mean foliage profiles within circular regions with varying horizontal ranges (radii) from the center point, ranging from 20 to 100 m. Hilker et al. (2010) showed that in a restricted geographic coverage (i.e., 30 × 30 m), foliage profiles from airborne discrete-return lidar match well with those from EVI. Here, we chose a circular-shaped pattern of areas of increasing horizontal range that better matches the spherical scanning of the EVI and the circular footprint of the airborne LVIS scanner.

2.3. Foliage profiles retrieved from EVI full-waveform data

For the EVI system, if the probability of canopy gap (hereafter referred to as Pgap) at the top of the canopy for a range of zenith angle rings is known, the LAI and vertical foliage profile can be readily obtained (Zhao et al., 2011). The mean profiles, excluding the zero zenith (or first ring) since it is the most variable, are averaged using the solid angles subtended by the rings as weighting.

Previous studies of the topographic effect on LAI estimated from vertically upward pointing hemispherical photographs have shown that slope increases the gap fraction downslope while it decreases gap fraction upslope. Walter and Torquebiau (2000) proposed replacing zenith angle θ with incidence angle γ (relative to the normal to the slope), which is defined as:

$$\cos\gamma = \cos\theta\cos\beta + \sin\theta\sin\beta\cos(\varphi - \varphi') \tag{4}$$

where θ is the zenith angle (relative to the flat ground), β is the ground slope, φ is the azimuth of incidence angle and φ' is the azimuth of ground slope. In this condition, the path length is no longer held constant for all azimuth directions.

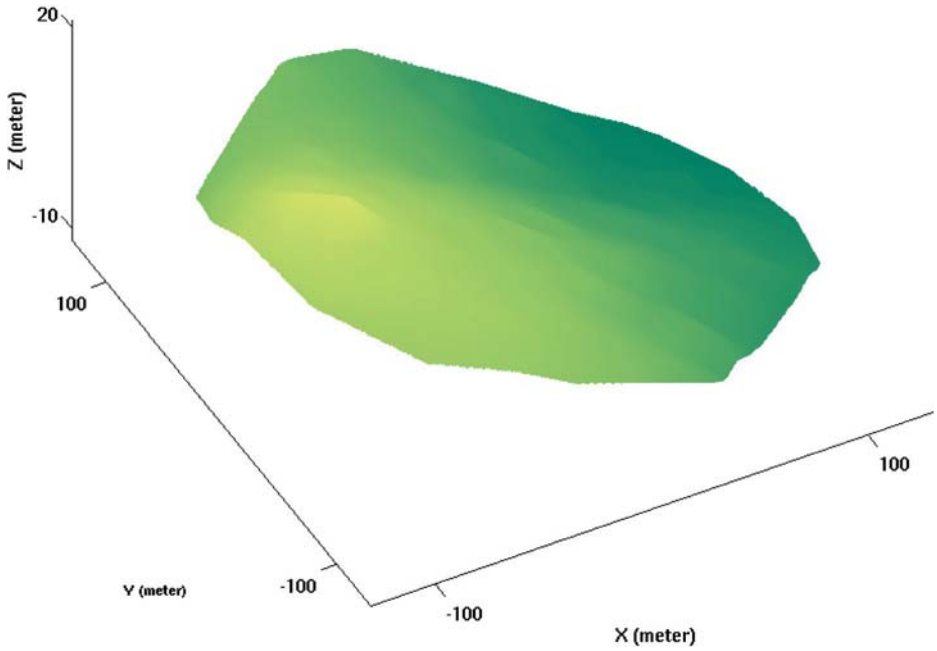

Fig. 4. DEM derived from LVIS waveforms. Green color from dark to light indicates height from low to high. (For interpretation of the references to color in this figure legend, the reader is referred to the web version of this article.)

To remove the local topographic effect on foliage profiles retrieved from the EVI full-waveform data, it is essential to identify how the ground returns fit along a regular slope. As these ground shots have somewhat unique characteristics (e.g. single returns, strong peak signatures, and primarily distributed in the lower hemisphere), they can be easily identified for further slope fitting. Once the single ground shots are identified with a form of point cloud, the slope can be fitted mathematically in 3-D space.

We fitted a least-squares plane to the elevation of the ground shots using an orthogonal distance regression that minimizes the sum of the distances of all points to the fitted plane. The slope and azimuth can then be derived based on the fitted equation.

$$Ax + By + Cz + D = 0 \tag{5}$$

where A, B and C are the components of the plane. Once the slope angle and azimuth angle were determined, we used the methodology proposed by Walter and Torquebiau (2000) to see how the foliage profile estimates were affected by local topography.

Compared with the MacArthur and Horn's (1969) method used to retrieve the foliage profiles, the gap fraction-based foliage retrieval profiles can only be processed at the scanning point level. To match the spatial scale, we can compare foliage profiles of a single center scan with those profiles obtained within a small spatial coverage area (e.g., 30 m in radius), while for larger spatial coverages, we need to use the mean foliage profile retrieved from five EVI scans to match the mean foliage profiles from LVIS within the same coverage.

2.4. Foliage profiles retrieved from EVI point cloud data

As opposed to airborne lidar scanning systems, with a fine spatial resolution and small beam size, terrestrial lidar systems can complement the weaknesses of airborne lidars by making a detailed characterization of the crowns in a small field site, making more accurate foliage profiles possible. For example, approximately 400,000 lidar pulses will exit the canopy over an area of 0.85 ha (assuming a 30-m canopy height) at varied view angles for EVI lidar scanning system. With 5 scans and about 2 million shots, nearly all the foliage region in 1-ha site will be well sampled. Also, more than 100,000 shots are directed to the ground from each scan, and as a result returned pulses from five merged scan can provide a quite detailed characterization of local topography (Fig. 5).

Although gap fractions can be obtained using a gap probability-based method at varying zenith regions or a gap fraction method over height (Hilker et al., 2010; Hosoi & Omasa, 2006), the foliage profile can also simply be retrieved from a point cloud using the following two expressions (Jupp et al., 2009).

$$f(z) = \frac{\partial\left(-\log\left(P_{gap}(z)\right)\right)}{\partial z} \tag{6}$$

where $P_{gap}(z)$ is the gap fraction measurement at height z; and $f(z)$ represents the foliage area volume density at height z. In this study, the gap fraction can be estimated as the total number of lidar hits up to a height z relative to the total number of lidar shots emitted out of the EVI instrument (Coops et al., 2007).

$$P_{gap}(z) = 1 - \frac{\sum_{z=1.7}^{z=j} \#Z_j}{N} \tag{7}$$

where $\#Z$ is the number of hits from the default EVI height 1.7-m up to a height z above the ground; N is the total number of shots emitted up to the sky. To avoid any hits that are intercepted by upslope local topography, only shots with zenith angles less than 85° were chosen.

Although the EVI can record hits beyond a 100-m range, most of the lidar shots are intercepted in a closer limited range, as shown in Fig. 1c, d. This is particularly true of the shots reflected back from the ground because the EVI instrument is mounted on a tripod at approximately 1.7 to 2.0 m. As a result, the best characterization of local topography is achieved by merging several EVI scans together.

To correct for the topographic effect on foliage profile retrievals from the EVI instrument, the ground points were first identified, and then fitted to a three-dimensional surface. The heights of other points were then adjusted accordingly using this 3-D surface.

The EVI point cloud used in this study is transformed directly from the EVI full-waveform data by identifying the waveform peaks within each single waveform as hits; each of the hits is then recorded with its geographic coordinates, which provides much more flexibility in retrieving foliage profiles with varying spatial coverages. To evaluate how the difference in scanning perspective impacts the foliage profile comparison, this study chose to provide the foliage profiles from varying circular regions, in the same way we retrieve mean foliage profile from LVIS. By investigating the foliage profile comparison at increasing circular ranges from a center point, a better understanding of the effect of the scanning perspective on the foliage profiles from these two sources is achieved.

3. Results

3.1. Foliage profiles retrieved from LVIS

Fig. 6 shows the LVIS-derived apparent foliage profiles as observed with circular ranges varying from 20 to 100 m for a single red fir site 305. Generally, the foliage profiles retrieved from closer horizontal ranges have relatively smaller FAVD values for the lower canopy (i.e. 12–18 m) and upper canopy (40–60 m), compared with those retrieved at longer ranges, while for the middle canopy (i.e. 30–40 m), they display a relatively higher FAVD. This variation demonstrates both the horizontal and vertical heterogeneity of the foliage distribution in this stand. Horizontally, as more single foliage profiles were averaged, the shape of mean foliage profiles became smoother, and this reflects a comprehensive view of this forest stand. Vertically, the canopy top heights of the foliage profiles retrieved at close ranges are higher than those of the foliage profiles at farther ranges, reflecting the mixed effect of slope and vertical heterogeneity over larger spatial regions. The difference in top height between the 20 m and 100 m ranges approaches 10 m, indicating the necessity of addressing the local topographic effects on the foliage profile retrievals, and also the need to match the foliage profiles spatially in a rigorous manner. Yang et al. (2011) assessed the generalized impacts of surface topography on vegetation lidar waveforms using an extended geometric optical and radiative transfer model. However, to remove the slope effect inherent in a single waveform obviously requires a more detailed description of forest structure and local topography.

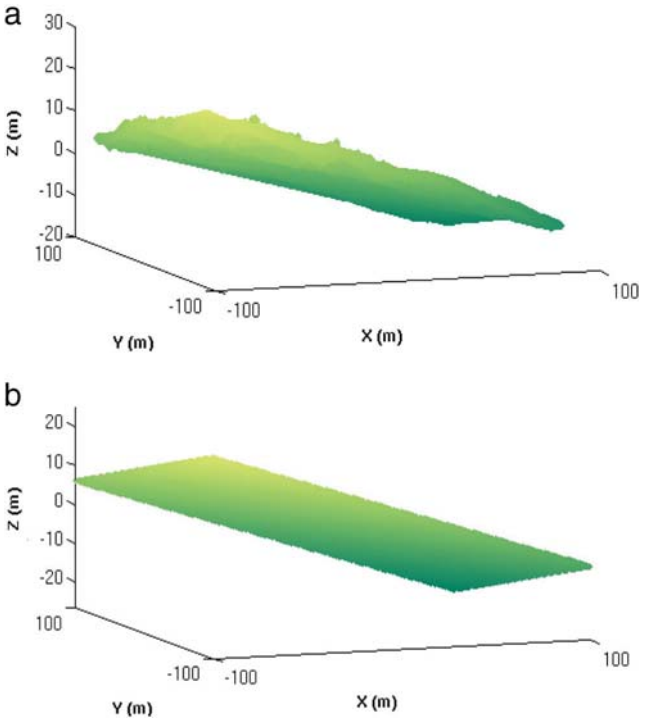

Fig. 5. Digital elevation model (DEM) derived from EVI point cloud. a) DEM derived from the EVI ground returns; b) fitted to a plane slope surface.

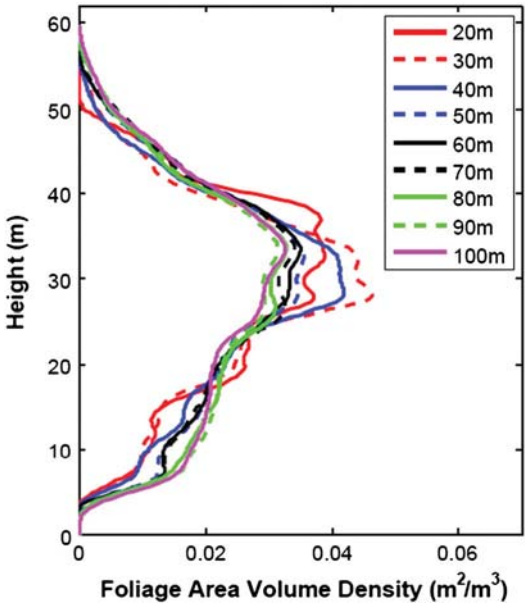

Fig. 6. LVIS-derived foliage profiles with varying spatial coverages, shown by horizontal radii (20–100 m) of coverage areas.

3.2. Foliage profiles retrieved from full-waveform EVI observations

Fig. 7a, b illustrates the specific local topographic effect on the foliage profiles for the center scan of the red fir site 305, and the mean of five scans respectively. Although a good agreement (i.e., $r = 0.977$; RMSE = 0.0025 for center scan, and $r = 0.991$; RMSE = 0.0015 for a mean of five scans) was found between the foliage profiles retrieved before the topographic correction and after the topographic correction for these two cases, foliage profiles derived from the center scan and the mean foliage profiles derived from five scans display an obvious topographic effect in terms of the shape of foliage profile and the topmost height. In particular, the peak at 10 m shrank greatly when the topographic correction was applied. In addition, the shape shifted approximately 2–3 m, and resulted in a topmost height that was 2–3 m higher than foliage profiles without the local topographic correction. Fewer variations were observed for the mean foliage profiles from the five scans because the local topographic effects were somewhat averaged among the five EVI scans. For example, the peak at the 18 m level was significantly reduced, and the topmost height also increased in the larger coverage.

3.3. Foliage profile retrieved from EVI point cloud

Fig. 8a, b demonstrates the effect of scanning perspective on foliage profiles derived from the EVI point cloud in two situations: before local topographic correction and after local topographic correction. The topmost height differences between these two situations increase over larger ranges, indicating the combined effect of the local topography and the spatial coverage. Another notable trend is that at closer ranges, the foliage profiles show smaller FAVD for the lower canopy (i.e. 10–15 m), and larger FAVD for the upper canopy (30–40 m) except at 20-m range. This can be explained by the fact that laser beams travel shorter distances before being intercepted at upper canopy level due to the high density of leaves, while the scattering events in the lower canopy tend to occur in the farther range due to lower density of leaves at this level. As a result, the horizontal ring setup tends to weight the upper canopy at closer ranges while for the lower canopy this effect is

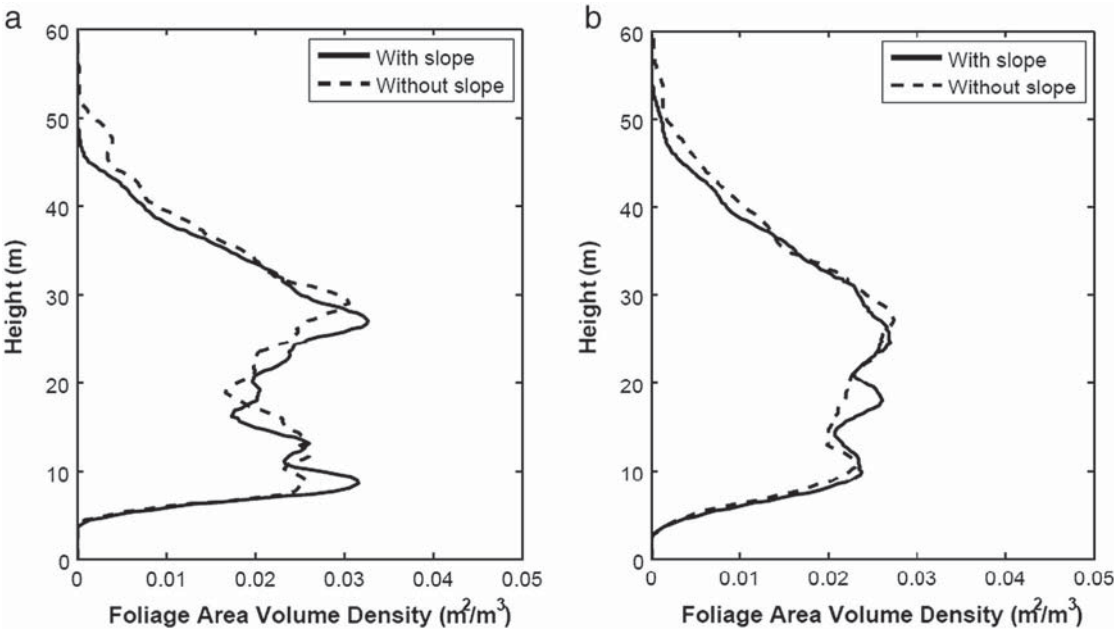

Fig. 7. Topographic effect on foliage profiles derived from EVI full-waveform data. a) Center scan; b) mean of five scans. With slope, before slope correction. Without slope, after slope correction.

dominated by scattering events occurring at farther range. The reason that this trend does not hold for 20 m range is probably due to a greatly clumped condition within the limited spatial coverage because EVI is usually located in a relatively open space.

The topmost heights only vary very slightly when local topography is not considered. This is because the tree topmost heights are higher in the downslope regions of red fir site 305 and this tends to mask the local topographic effect somewhat. When the local topography is removed, the higher trees in the downslope are represented more appropriately.

3.4. Foliage profile comparison

Figs. 9 and 10 compare the foliage profiles retrieved from the following three sources: EVI full-waveform, EVI point cloud and LVIS. Two cases are considered for each data source: before a local topographic correction and after a local topographic correction. For most horizontal ranges, the foliage profiles retrieved from LVIS reveal higher topmost canopy heights than those retrieved from EVI. This reflects the fact that the airborne LVIS system, looking down from above, tends to characterize the canopy tips of the dominant trees more accurately while the terrestrial lidar system may miss the canopy tips of many of the dominant trees due to occlusion. This of course depends on the location of scanning point, and the forest tree density. In addition, LVIS-derived foliage profiles all demonstrate a higher upper canopy peak (at a height of 30–40 m) than those retrieved from EVI point cloud, due to the fact that LVIS recorded footprints illuminated within a $\pm 7°$ field of view while a nadir view was assumed in deriving foliage profile from EVI point cloud. Compared with the LVIS-derived foliage profiles, the upward looking EVI system samples the lower part of the forest stand

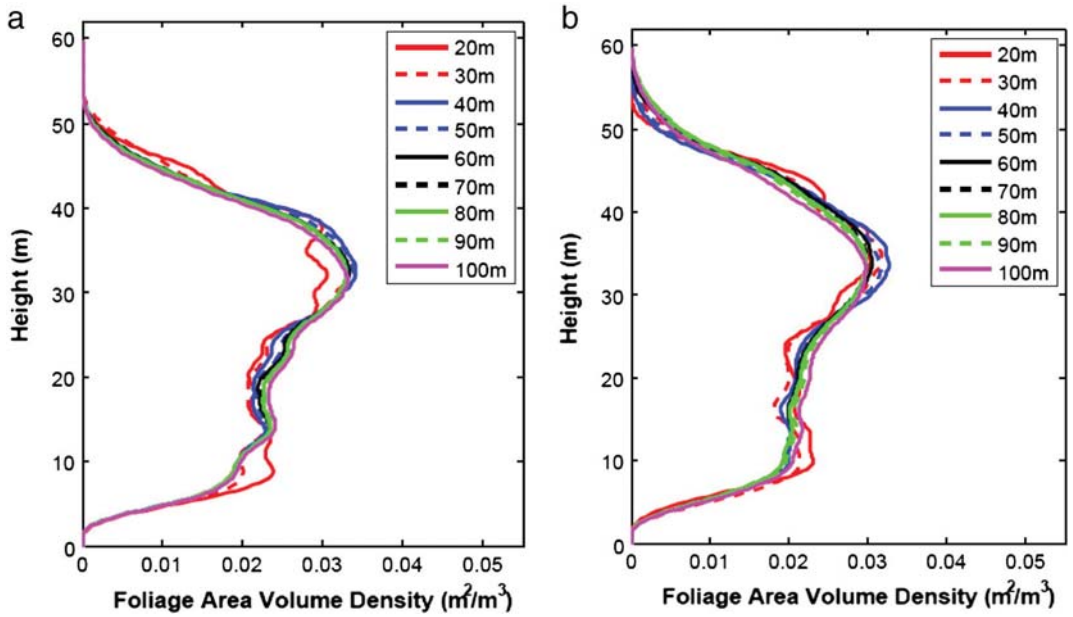

Fig. 8. Foliage profiles by spatial coverage area radii using the EVI point cloud. a) Before slope correction; b) after slope correction.

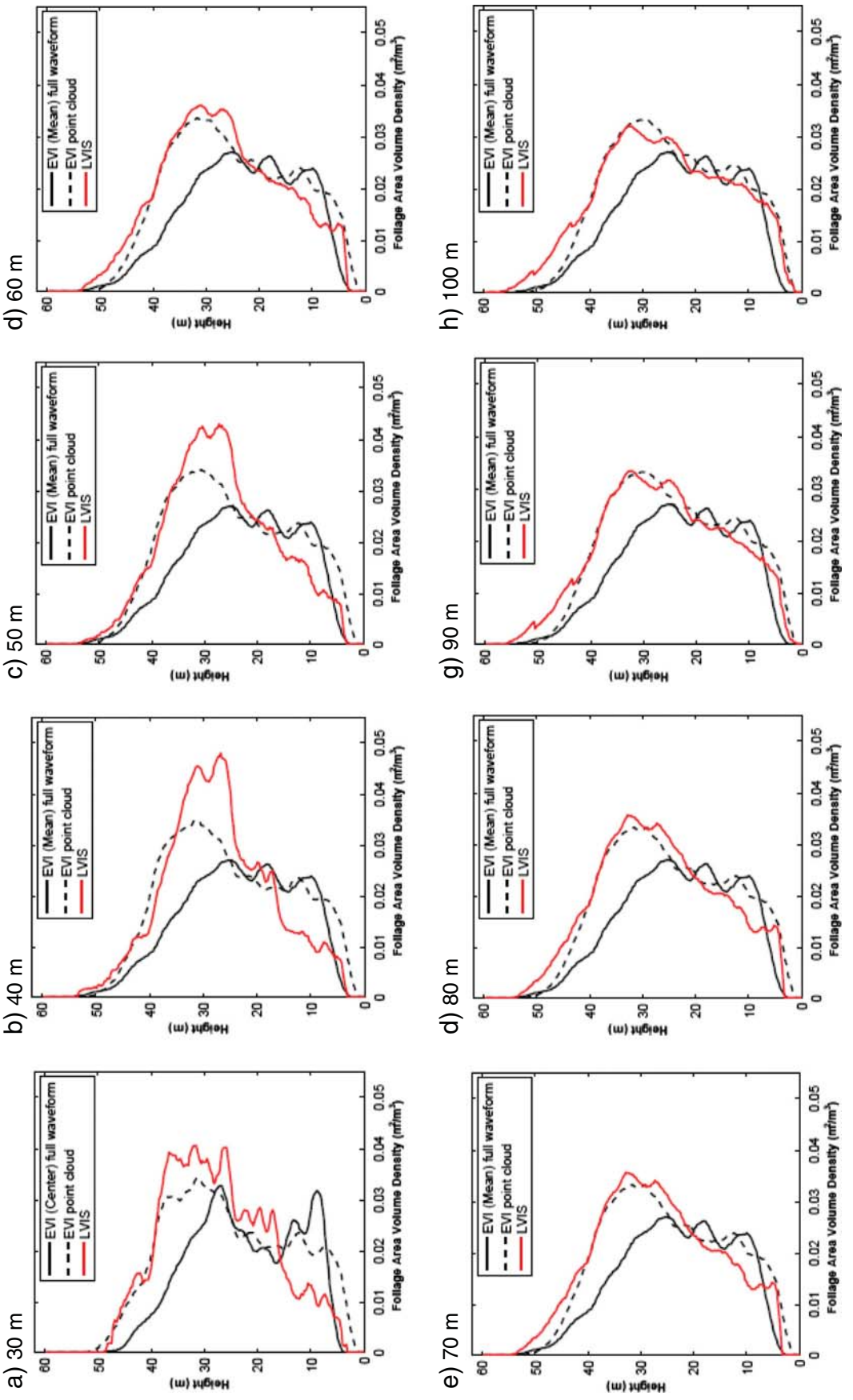

Fig. 9. Foliage profile comparisons at varying horizontal ranges from the center before slope correction.

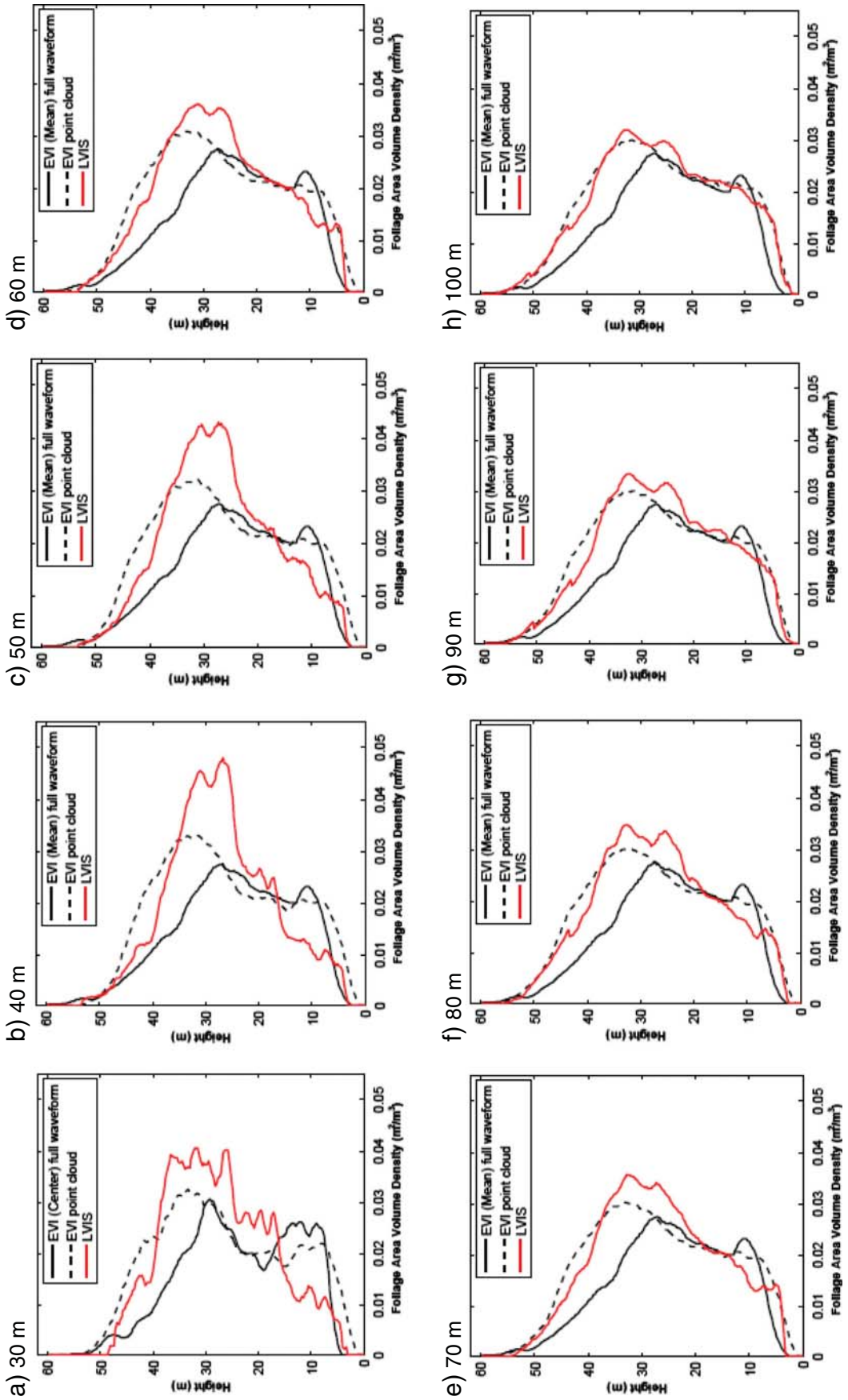

Fig. 10. Local topography corrected foliage profile comparisons at varying horizontal ranges from the center after slope correction.

more accurately, and thus may miss some of the top canopy part in the farther ranges, retrieving a lower FAVD for the upper canopy.

Therefore, foliage profiles derived from the EVI full-waveform data all show higher FAVD for the lower canopy. The difference is caused primarily by the fact that the gap fractions are calculated for the maximum range, and as a result, more interceptions are contributing to the retrieved foliage profiles, leading to a higher peak in the lower part of the canopy. As the horizontal ranges increase, the foliage profiles retrieved from EVI full waveform correlate better, with r increasing from 0.74 at 30 m to 0.92 at 100 m of horizontal distance.

Foliage profiles from EVI point clouds agreed well with those from the LVIS system at all horizontal distances, but particularly in the farther range (e.g., $r = 0.987$ at 100 m horizontal distances). Note that the foliage profiles from the EVI point cloud are more similar to those retrieved from LVIS, and are therefore actually apparent foliage profiles that are based on limited sampled zeniths. In contrast, the foliage profiles from the EVI full-waveform data and those from the LVIS differ not only because of their different viewing directions, but also because of differences in the regions that are sampled. These comparisons suggest that the different methodologies used for foliage profile retrieval play an important role in the variation among foliage profiles retrieved from varied sources.

After slope correction, the foliage profiles retrieved using the three methods display a similar pattern, as shown in Fig. 10. However, it obviously improves the correlation of foliage profiles from the EVI full waveform and the EVI point cloud, implying a critical need to remove local topographic effects before making foliage profile comparisons. The lower correlation between the profiles retrieved from LVIS and those retrieved from EVI point clouds also emphasizes the importance of correcting the local topography in the retrieval of foliage profiles at the shorter horizontal ranges.

Fig. 11a, b shows the effect of the scanning perspective on the foliage profile retrieval. Relatively lower correlations were observed for the smaller horizontal ranges (i.e., distance from center is less than 30 m). This may be due in part to the inherent errors in identifying the center points with the GPS devices. The local topographic effect also plays a

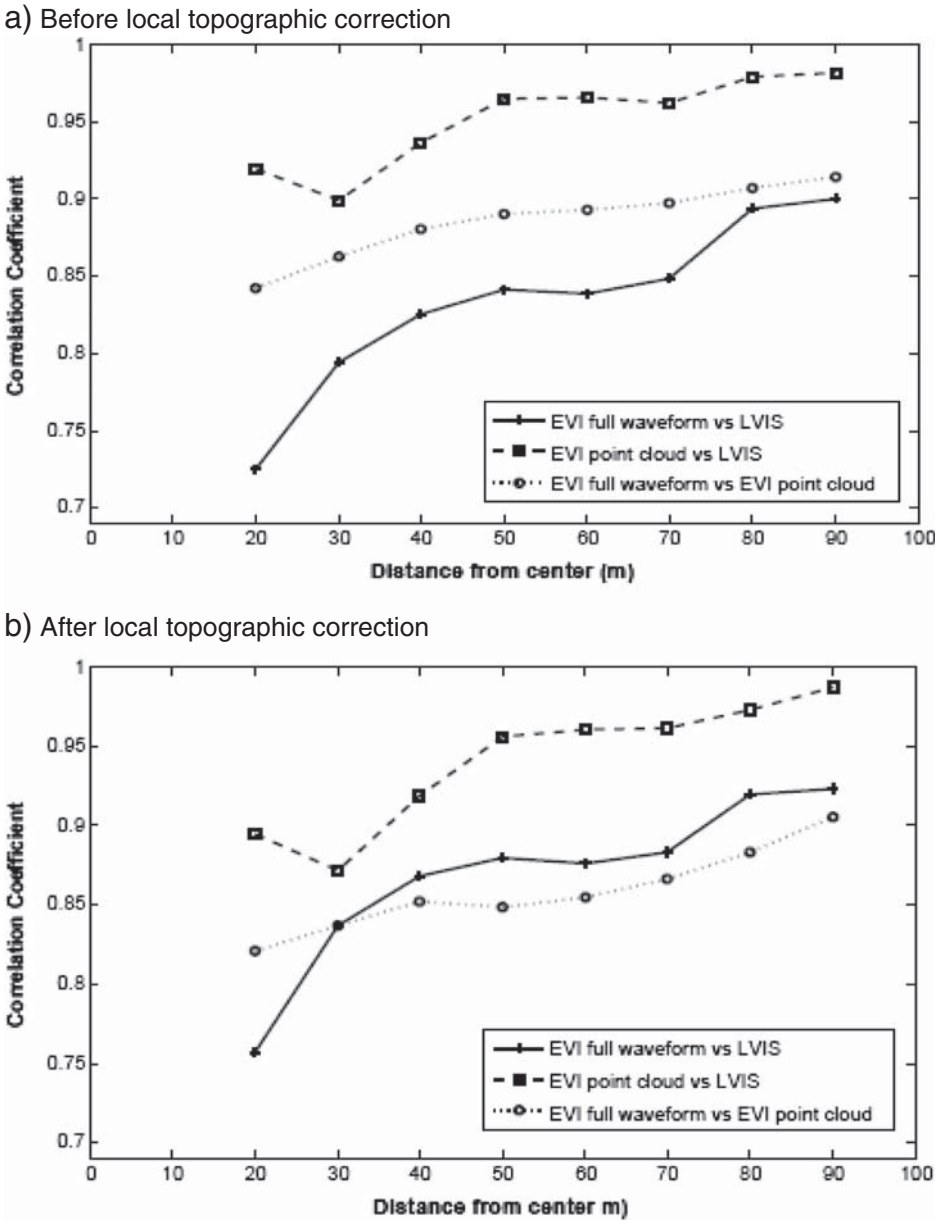

Fig. 11. Correlation coefficient comparisons at varying horizontal ranges. a) Before local topography correction; b) after local topography correction.

role. After the slope correction, the foliage profiles retrieved from the EVI full wave forms show a better correspondence with LVIS data than before the topographic correction, implying that the effects of topography at between-footprint scales had been removed, and consideration of the within-footprint topographic effects may provide more accurate foliage profiles from LVIS system.

4. Discussion and conclusions

This paper assesses the agreement between foliage profiles retrieved from the airborne LVIS lidar scanning system with those retrieved from the terrestrial Echidna lidar scanning system over varying horizontal distances from the site center, and over complex local topography. Airborne or spaceborne lidar scanning systems are attractive for mapping foliage profiles at regional and even continental scales because they can achieve larger spatial coverage, but they are limited by only capturing a near-nadir view and by an inability to characterize the detailed local topography. The comparison of foliage profiles from the lower spatial resolution, downward-looking airborne LVIS lidar scanning system with the very highly sampled, upward-looking terrestrial EVI scanning system provides a better understanding of the limitations of airborne lidar systems, as well as the mechanisms leading to the mismatch.

This study reveals that view perspective, local topography, and spatial coverage are the main external factors that cause a mismatch of foliage profiles from these two lidar systems. We investigated the local topographic effect and spatial coverage effect on foliage profile retrievals from three data sources: the EVI full-waveform data, the EVI point cloud, and the LVIS. We found that the correct characterization of topmost height was strongly affected by local topography, while the lower canopy and middle canopy correlated well regardless of whether the data had been topographically corrected or not. This finding suggests that height metrics retrieved from the LVIS system may need to consider the effect of local topography more carefully. With respect to the effect of scanning perspective, we have shown that in making direct comparisons of foliage profiles retrieved from small areas, the areas need to be closely matched, given GPS errors. With increasing area of spatial coverage (increasing horizontal range), the forests are sampled more evenly, and this results in profiles that are more similar.

Our work shows the benefits of using the detailed description of forest canopy structure retrieved from terrestrial lidar systems in mapping foliage profiles over larger areas. As suggested by Ni-Meister et al. (2008), using a Geometric-Optical and Radiative-Transfer (GORT) model, relating both above-canopy and below-canopy lidar measurements may be expected to improve retrievals of forest canopy structure information, such as the foliage profile. With the help of terrestrial lidar, the negative impact of topography and the limited sampling region of foliage profiles can be minimized.

Some similar findings have previously been reported by Hilker et al. (2010), who found good agreement between foliage profiles measured with EVI and airborne small-footprint foliage profiles in four plots of boreal forest stands, although the airborne foliage profiles showed generally less foliage in the middle and lower canopies.

Our study has explored the comparison of foliage profiles between terrestrial and airborne large-footprint lidar systems by taking the effect of local topography, view perspective, and spatial coverage into account at a site dominated by sparsely distributed trees.

The good agreement of foliage profile retrievals between EVI point cloud and the LVIS does not indicate that airborne measured foliage profiles are more accurate than those from EVI full waveform. Rather it suggests that the differences in the foliage profiles derived from the EVI full waveform data and LVIS system are mostly due to the way these two systems sample the forest. Although airborne lidar systems have proven useful in retrieving foliage area profiles, they are limited by their nadir view; moreover, they must of necessity assume a predetermined leaf orientation (G function) or assume random leaf orientation, while the full-waveform EVI data provides a pathway to correct for G function effects. With a fine spatial resolution and a small beam size, terrestrial lidar systems complement the strengths of the airborne lidars by making a detailed characterization of the crowns from a small field site, thereby serving as a calibration tool and providing localized tuning information for future airborne and spaceborne lidar missions.

Acknowledgments

This research was supported by NASA under grants NNG06GI92G and NNX08AE94A and NSF under grant MRI-0923389. The authors gratefully acknowledge the assistance of Mitchell Schull, Pontus Olofsson, Mary LeeAnn King, Sage Sheldon, Amanda Sharon Whitehurst, Anupam Anand and Anuradha Swatantran at Sierra National Forest sites. We are also grateful to the many suggestions made by reviewers that significantly improved our paper.

References

Blair, J. B., Hofton, M. A., & Rabine, D. L. (2006). Processing of NASA LVIS elevation and canopy (LGE, LCE and LGW) data products, version 1.01. Available at http://lvis.gsfc.nasa.gov

Blair, J. B., Rabine, D. L., & Hofton, M. A. (1999). The Laser Vegetation Imaging Sensor (LVIS): A medium-altitude, digitization-only, airborne laser altimeter for mapping vegetation and topography. *ISPRS Journal of Photogrammetry and Remote Sensing*, *54*, 115–122.

Coops, N. C., Hilker, T., Wulder, M. A., St-Onge, B., Newnham, G., Siggins, A., et al. (2007). Estimating canopy structure of Douglas fir forest stands from discrete-return LiDAR. *Trees Structure Function*, *21*, 295–310.

Drake, J. B., Dubayah, R. O., Knox, R. G., Clark, D. B., & Blair, J. B. (2002). Sensitivity of large-footprint lidar to canopy structure and biomass in a neotropical rainforest. *Remote Sensing of Environment*, *81*, 378–392.

Harding, D. J., Lefsky, M. A., Parker, G. G., & Blair, J. B. (2001). Laser altimeter canopy height profiles: Methods and validation for deciduous, broadleaf forests. *Remote Sensing of Environment*, *76*(3), 283–297.

Hilker, T., van Leeuwen, M., Coops, N. C., Wulder, M. A., Newnham, G. J., Jupp, D. L. B., et al. (2010). Comparing canopy metrics derived from terrestrial and airborne laser scanning in a Douglas-fir dominated forest stand. *Trees*. http://dx.doi.org/10.1007/s00468-010-0452-7.

Hosoi, F., & Omasa, K. (2006). Voxel-based 3-D modeling of individual trees for estimating leaf area density using high resolution portable scanning lidar. *IEEE Transcations on Geoscience and Remote Sensing*, *44*(12), 3610–3618.

Hosoi, F., & Omasa, K. (2007). Factors contributing to accuracy in the estimation of the woody canopy leaf-area-density profile using 3D portable lidar imaging. *Journal of Experimental Botany*, *58*(12), 3464–3473.

Jupp, D. L. B., Culvenor, D. S., Lovell, J. L., Newnham, G. J., Strahler, A. H., & Woodcock, C. E. (2009). Estimating forest LAI profiles and structural parameters using a ground based laser called "Echidna®". *Tree Physiology*, *29*(2), 171–181.

Kotchenova, S. Y., Song, X., Shabanov, N. V., Potter, C. S., Knyazikhin, Y., & Myneni, R. B. (2004). Lidar remote sensing for modeling gross primary production of deciduous forests. *Remote Sensing of Environment*, *92*(2), 158–172.

Lee, S., Ni-Meister, W., Yang, W., & Chen, Q. (2011). Physically based vertical vegetation structure retrieval from ICESat data: Validation using LVIS in White Mountain National Forest, New Hampshire, USA. *Remote Sensing of Environment*, *115*(11), 2776–2785.

Lefsky, M. A. (1997). *Application of lidar remote sensing to the estimation of forest canopy and stand structure.* (PhD dissertation). Charlottesville, VA: University of Virginia.

Lefsky, M., Cohen, W., Acker, S., Parker, G., Spies, T., & Harding, D. (1999). Lidar remote sensing of biophysical properties and canopy structure of forests of Douglas-fir and western hemlock. *Remote Sensing of Environment*, *70*(3), 339–361.

MacArthur, R. H., & Horn, H. S. (1969). Foliage profile by vertical measurements. *Ecology*, *50*, 802–804.

Ni-Meister, W., Jupp, D. W. B., & Dubayah, R. (2001). Modeling lidar waveforms in heterogeneous and discrete canopies. *IEEE Transactions on Geoscience and Remote Sensing*, *39*(9), 1943–1958.

Ni-Meister, W. A., Strahler, A. H., Woodcock, C. E., Schaff, C., Jupp, D. L. B., Yao, T., et al. (2008). Modeling the hemispherical scanning, below-canopy lidar and vegetation structure characteristics with a geometric optical and radiative transfer model. *Canadian Journal of Remote Sensing*, *34*(s2), 385–397.

Parker, G. G., Lefsky, M. A., & Harding, D. J. (2001). PAR transmittance in forest canopies determined from airborne lidar altimetry and from in-canopy quantum measurements. *Remote Sensing of Environment*, *76*, 298–309.

Stark, S. C., Leitold, V., Wu, J. L., Hunter, M. O., Castilho, C. V. D., Costa, F. R. C., et al. (2012). Amazon forest carbon dynamics predicted by profiles of canopy leaf area and light environment. *Ecology Letters*, *15*(12), 1406–1414.

Strahler, A. H., Jupp, D. L. B., Woodcock, C. E., Schaaf, C. B., Yao, T., Zhao, F., et al. (2008). Retrieval of forest structure parameters using a ground based laser Instrument (Echidna®). *Special issue for Canadian Journal of Remote Sensing*, *34*(2), 426–440.

Sun, G., Ranson, K. J., Kimes, D. S., Blair, J. B., & Kovacs, K. (2008). Forest vertical structure from GLAS: An evaluation using LVIS and SRTM data. *Remote Sensing of Environment*, *112*(1), 107–117.

Tang, H., Dubayah, R., Swatantran, A., Hofton, M., Sheldon, S., Clark, D. B., et al. (2012). Retrieval of vertical LAI profiles over tropical rain forests using waveform lidar at La Selva, Costa Rica. *Remote Sensing of Environment*, *124*, 242–250.

Toda, M., Yokozawa, M., Sumida, A., Watanabe, T., & Hara, T. (2009). Foliage profiles of individual trees determine competition, self-thinning, biomass, and NPP of a Cryptomeria Japonica forest stand: A simulation study based on a stand-scale process based forest model. *Ecological Modeling*, *2272–2280*.

Walter, J-. M. N., & Torquebiau, E. F. (2000). The computation of forest leaf area index on slope using fish-eye sensors. *Comptes Rendus de l'Acade´mie des Sciences, Se´ rieIII Sciences de la Vie*, *323*, 801–813.

Wilson, J. W. (1965). Stand structure and light penetration. I. Analysis by point quadrats. *Journal of Applied Ecology*, *2*, 383–390.

Wilson, J. W. (1960). Inclined point quadrats. *New Phytologist*, *59*, 1–8.

Wilson, J. W. (1963). Estimation of foliage denseness and foliage angle by inclined point quadrats. *Australian Journal of Botany*, *11*, 95–105.

Yang, W., Ni-Meister, W., & Lee, S. (2011). Assessment of the impacts of surface topography, off-nadir pointing and vegetation structure on vegetation lidar waveforms using an extended geometric optical and radiative transfer model. *Remote Sensing of Environment*, *115*(11), 2810–2822.

Yao, T., Yang, X., Zhao, F., Wang, Z., Zhang, Q., Jupp, D. L. B., et al. (2011). Measuring forest structure and biomass in New England forest stands using Echidna® ground-based lidar. *Remote Sensing of Environment*, *115*(11), 2965–2974.

Zhao, F., Yang, X., Schull, M. A., Roman-colon, M. O., Yao, T., Wang, Z., et al. (2011). Measuring leaf area index, foliage profile, and stand height in New England Forest stands using Echidna® ground-based lidar. *Remote Sensing of Environment*, *115*(11), 2954–2964.